

Prediction and experimental validation of cutting forces in ball end milling of aluminum 7075-T6 alloy

Mekentichi Sifeddine^{1*}, Brahim Benmohammed¹ , Daniel Schlegel², Sora Lee-Remond³, Ahmed Benyoucef⁴

¹ Product Research Laboratory, Faculty of Technology, Mechanical Engineering Department, University Batna 2 - Mostefa Benboulaïd, 53 Route de Constantine, Fésdis, Batna 05078, Algeria

² University Institute of Technology, University of Haute-Alsace, Mulhouse, France

³ École Supérieure des Technologies et des Affaires (ESTA), Université Marie et Louis Pasteur, ELLIADD Laboratory (U.R. No. 4661), Belfort, France

⁴ Higher National School of Renewable Energies, Environment & Sustainable Development, Constantine road, Fesdis, Batna, 05078, Algeria

* Corresponding author's e-mail: s.mekentichi@univ-batna2.dz

ABSTRACT

This study presents the development and validation of a hybrid cutting force prediction model for ball end milling of aluminum 7075-T6 alloy. The model combines a mechanistic approach with a specific cutting force coefficient ($K_s = 850 \text{ N/mm}^2$) sourced from experimental literature. Cutting forces in the x, y, and z directions are predicted by integrating differential force components with tool geometry and machining parameters. Experimental validation was performed under dry conditions at a spindle speed of 15,000 rpm. In the x-direction, the simulated force was 162.4 N versus an experimental force of 215.4 N; in the y and z-directions, predicted values (65.2 N and 25.3 N) closely matched experimental forces (74.3 N and 28.2 N), respectively. The corresponding mean absolute errors were 18.2% (x), 4.5% (y), and 3.3% (z). The higher error in the x direction highlights limitations in modeling tangential force dynamics, while the y and z predictions align closely with experimental data. Leveraging the experimentally derived K_s , the proposed model offers a practical tool for optimizing machining processes in the

aerospace sector, with potential for further refinement in tangential force modeling.

Keywords: cutting forces, ball end milling, aluminum 7075-T6 alloy, machining parameters, experimental validation.

INTRODUCTION

The accurate prediction of cutting forces is fundamental to enhancing productivity, tool life, and process stability in modern machining operations. Ball end milling, in particular, is indispensable for producing sculpted surfaces, mold cavities, and aerospace components, where precision and surface integrity are paramount [1, 2]. The

process becomes increasingly complex at high spindle speeds, as cutting forces are influenced by intricate interactions among tool geometry, cutting conditions, and material behavior. This complexity makes reliable force prediction both a technical challenge and an industrial necessity [3, 4]. Aluminum 7075-T6 alloy has emerged as a material of choice in aerospace and high performance engineering due to its exceptional strength-to-weight ratio, good fatigue resistance, and favorable machinability [5, 6]. However, its relatively high hardness and low thermal conductivity can accelerate tool wear and cause significant variation in cutting forces during machining, especially under demanding conditions. These challenges underscore the importance of accurate force prediction not only for optimizing cutting parameters but also

for maintaining dimensional accuracy, reducing tool wear, and ensuring consistent product quality [7, 8]. A variety of models have been developed to estimate cutting forces in milling. Mechanistic models, which relate chip load to cutting forces via material and tool dependent coefficients, are widely adopted for their sound physical basis and computational efficiency [9]. These models typically decompose forces into tangential, radial, and axial components, with cutting force coefficients reflecting the influence of tool geometry, material properties, and machining parameters. However, conventional mechanistic models often fall short in ball end milling applications, where the continuously varying chip thickness and tool engagement angles along the toolpath introduce significant modeling challenges [10]. As a result, their predictive accuracy diminishes in scenarios involving complex surface geometries or high speed operations [11, 12].

To address these limitations, recent research has focused on hybrid modeling strategies that combine mechanistic formulations with empirical calibration [13]. By integrating experimentally determined cutting force coefficients, these models can better capture the nonlinear and material specific interactions that occur in challenging machining scenarios, such as the high speed milling of aluminum 7075-T6 alloy [14, 15]. For example, models that account for the influence of tool orientation, chip thickness variation, and process dynamics have demonstrated improved accuracy in predicting cutting forces for complex surfaces [16]. Despite these advances, there remains a lack of comprehensive studies that systematically validate such models for ball end

milling of aluminum 7075-T6 alloy under realistic industrial conditions, particularly with respect to the effects of tool geometry, entry/exit angles, and uncut chip thickness variation [17, 18].

Motivated by these gaps, this study proposes a hybrid mechanistic model for predicting cutting forces in ball end milling of aluminum 7075-T6 alloy. The model is grounded in the classical decomposition of forces and incorporates a specific cutting force coefficient ($K_s = 850 \text{ N/mm}^2$), as established in prior experimental studies. Experimental validation was performed using a CNC milling machine and a Kistler 9257A dynamometer to measure forces along the x, y, and z axes. The predicted forces were compared with experimental data to evaluate model accuracy and to identify key sources of error.

This work is guided by the research question: How can a hybrid mechanistic model improve the prediction of cutting forces in ball end milling of aluminum 7075-T6 alloy? By addressing this question, the study aims to bridge the gap between theoretical modeling and experimental validation, providing a robust and practically relevant method for force prediction. The insights gained are expected to advance understanding of force generation mechanisms in complex milling operations and support improved process planning, toolpath design, and machining strategy development for high performance materials such as aluminum 7075-T6 alloy.

MECHANISTIC CUTTING FORCE MODEL

In the mechanistic approach to cutting force modeling, the differential cutting force on an

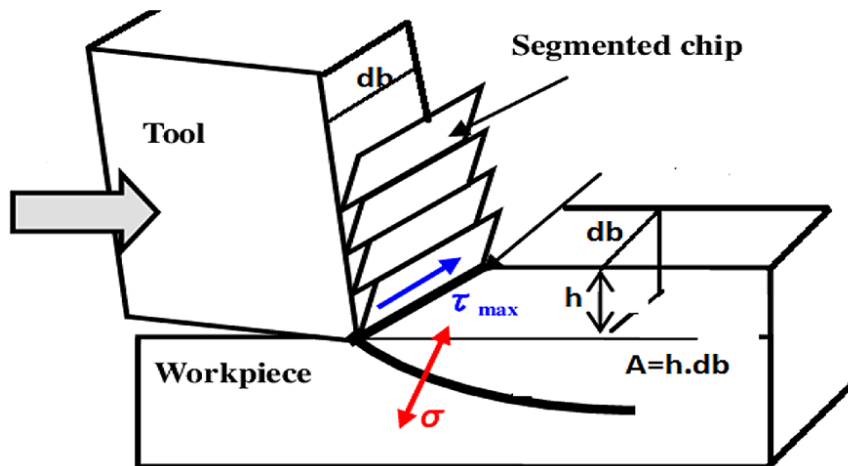


Figure 1. Representation of the chip area (A), chip thickness (h), width of cut (db)

infinitesimal segment of the cutting edge are depicted in Figure 1 and expressed by Equation 1:

$$dF = K_s \cdot h \cdot db \quad (1)$$

where: dF – differential cutting force (N), K_s – specific cutting force coefficient (N/mm²), h – instantaneous chip thickness (mm), db – differential width of cut (mm).

This model predicts the total cutting forces F_x , F_y , and F_z in the tool coordinate system by decomposing, transforming, and integrating these differential contributions. The differential forces are already defined as:

$$\begin{pmatrix} dF_t \\ dF_r \\ dF_a \end{pmatrix} = h \cdot db \begin{pmatrix} k_t \\ k_r \\ k_a \end{pmatrix} \quad (2)$$

where: dF_t – tangential differential force (N), dF_r – radial differential force (N), dF_a – axial differential force (N), k_t – tangential specific force coefficient (N/mm²), k_r – radial specific force coefficient (N/mm²), k_a – axial specific force coefficient (N/mm²).

In this model k_t , k_r , and k_a are used as provided values, with their derivation from $K_s = 850$ N/mm² implicitly established through experimental calibration specific to this material (aluminum 7075-T6 alloy) [19, 20].

Local force components

The differential forces are already defined as:

$$\begin{aligned} dF_t &= k_t \cdot h \cdot db \\ dF_n &= k_n \cdot h \cdot db \\ dF_a &= k_a \cdot h \cdot db \end{aligned} \quad (3)$$

These forces are in the local coordinate system of the cutting edge, and their magnitudes depend on $h(\phi)$, which varies with the cutting angle θ due to the ball-end mill's geometry.

Projection into the tool coordinate system

The rotation matrix T transforms the local forces into the global coordinates system. The matrix T accounts for tool rotation, aligning force components with the milling coordinate system, ensuring accurate force prediction across varying cutting angles. The matrix T given by:

$$[T] = \begin{pmatrix} -\cos(\phi) & -\sin(\phi) & 0 \\ \sin(\phi) & -\cos(\phi) & 0 \\ 0 & 0 & 1 \end{pmatrix} \quad (4)$$

where: ϕ – tool rotation angle (radians).

The general form of the global cutting force components is expressed as follow:

$$\{dF\} = [T] \cdot \begin{bmatrix} dF_t \\ dF_r \\ dF_a \end{bmatrix} = \begin{pmatrix} -\cos(\phi) & -\sin(\phi) & 0 \\ \sin(\phi) & -\cos(\phi) & 0 \\ 0 & 0 & 1 \end{pmatrix} \cdot \begin{bmatrix} k_t \cdot h \cdot db \\ k_n \cdot h \cdot db \\ k_a \cdot h \cdot db \end{bmatrix} \quad (5)$$

$$\begin{aligned} dF_x &= -dF_t \cdot \cos(\phi) - dF_n \cdot \sin(\phi) \\ dF_y &= dF_t \cdot \sin(\phi) - dF_n \cdot \cos(\phi) \\ dF_z &= dF_a \end{aligned} \quad (6)$$

Substituting the local force expressions:

$$\begin{aligned} dF_x &= -(k_t \cdot h \cdot db) \cdot \cos(\phi) - (k_n \cdot h \cdot db) \cdot \sin(\phi) \\ dF_y &= (k_t \cdot h \cdot db) \cdot \sin(\phi) - (k_n \cdot h \cdot db) \cdot \cos(\phi) \\ dF_z &= k_a \cdot h \cdot db \end{aligned} \quad (7)$$

Integration over the cutting edge

The global forces F_x , F_y , and F_z are computed by integrating the differential forces over the engaged cutting edge, from θ_{entry} to θ_{exit} .

For a rotating tool, $db = R \cdot d\theta$ (where R is the tool radius), and $h(\theta) = f_t \cdot \sin(\theta)$ varies with θ . The integrals are:

$$\begin{aligned} F_x &= \int_{\theta_{entry}}^{\theta_{exit}} [-k_t \cdot h(\theta) \cdot \cos(\phi) - k_n \cdot h(\theta) \cdot \sin(\phi)] \cdot R d\theta \\ F_y &= \int_{\theta_{entry}}^{\theta_{exit}} [k_t \cdot h(\theta) \cdot \sin(\phi) - k_n \cdot h(\theta) \cdot \cos(\phi)] \cdot R d\theta \\ F_z &= \int_{\theta_{entry}}^{\theta_{exit}} [k_a \cdot h(\theta)] \cdot R d\theta \end{aligned} \quad (8)$$

Numerical summation

For numerical computation, the cutting edge is discretized into N elements:

$$\begin{aligned} F_x &= \sum_{i=1}^N [-k_t \cdot h(\theta_i) \cdot \cos(\phi) - k_n \cdot h(\theta_i) \cdot \sin(\phi)] \cdot \Delta b \\ F_y &= \sum_{i=1}^N [k_t \cdot h(\theta_i) \cdot \sin(\phi) - k_n \cdot h(\theta_i) \cdot \cos(\phi)] \cdot \Delta b \\ F_z &= \sum_{i=1}^N [k_a \cdot h(\theta_i)] \cdot \Delta b \end{aligned} \quad (9)$$

where: Δb –width of each discrete element, θ_i – angular position of the i -th element.

SIMULATION RESULTS

This study utilizes a 4 mm axial depth of cut to investigate the cutting forces during an up-milling operation, characterized by 30% radial immersion, a zero-degree start angle, and a 66.4° exit angle. The cutting force coefficients are assumed uniform across all four teeth of the tool, with the work piece consisting of aluminum 7075-T6 alloy. The simulation incorporates the cutting parameters outlined in Table 1. Figure 2 represents the components of simulated cutting forces as a function vs. time:

The simulated cutting forces fluctuate across all three axes due to variations in the ball surface normal angle. These changes affect the axial, tangential, and radial force components, stemming from the tool’s engagement, with the work piece at different positions along its spherical surface. This interaction shifts as the ball surface normal angle varies.

Table 1. Cutting parameters values

Cutting parameters	Values
Cutting tool	12 mm diameter and 4 fluted Ball-End
Helix angle	30°
Force angle	60°
Feed rate	3000 (mm/min)
Spindle speed	15000 (rpm)
Specific force (aluminum 7075-T6 alloy)	850 (N/mm ²)

EXPERIMENTAL METHODOLOGY

This study combined experimental milling tests with a mechanistic simulation to predict and validate cutting forces in ball end milling of aluminum 7075-T6 alloy. The methodology involved precise force measurements under controlled conditions and a computational model to replicate these forces, enabling a robust comparison. Milling operation utilized a carbide ball-end milling cutter, chosen for its exceptional hardness and wear resistance, ideal for high-speed machining of aluminum 7075-T6 alloy with precision and efficiency. The cutter had a 12 mm diameter, four flutes, and a 30° helix angle.

The milling experiments conducted using the SOMAB DIAM 850 CNC machine tool presented in Figure 3. This machine provides a spacious working area, with an x-axis travel of 850 mm, a y-axis travel of 600 mm, and a z-axis travel of 560 mm, accommodating diverse milling tasks. Its spindle, capable of reaching 15000 rpm with a 15 kW power rating, enables high-speed milling under varied cutting conditions.

Cutting forces were measured using a Kistler 9257A dynamometer paired with a Kistler 5017B charge amplifier to ensure high-fidelity data, as shown in Figure 4a and 4b, respectively. This system enabled precise force measurements critical for validating the mechanistic cutting force model.

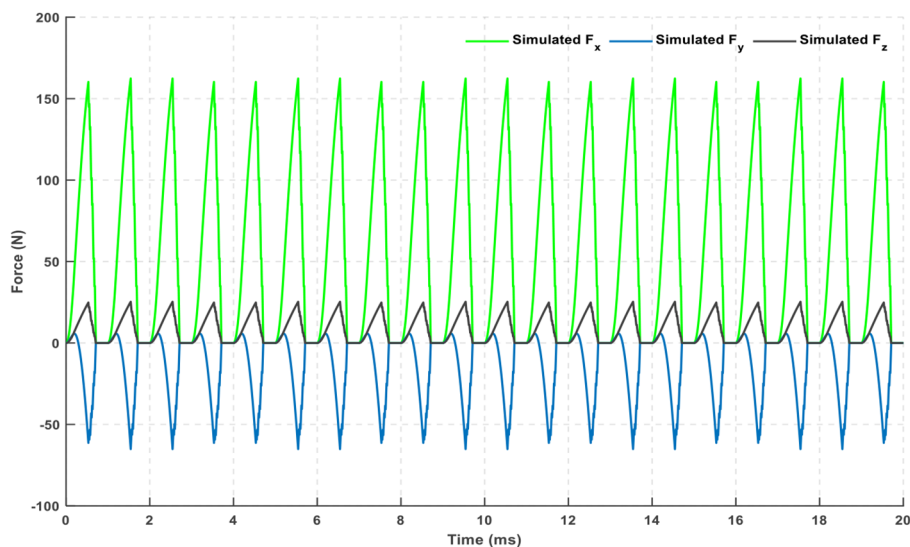


Figure 2. Ball end-milling simulated cutting forces for aluminum 7075-T6 alloy



Figure 3. SOMAB DIAM 850 CNC machine tool, TITAN Platform of the UTBM-Industry 4.0 Pole, (Belfort - Montbéliard, France)

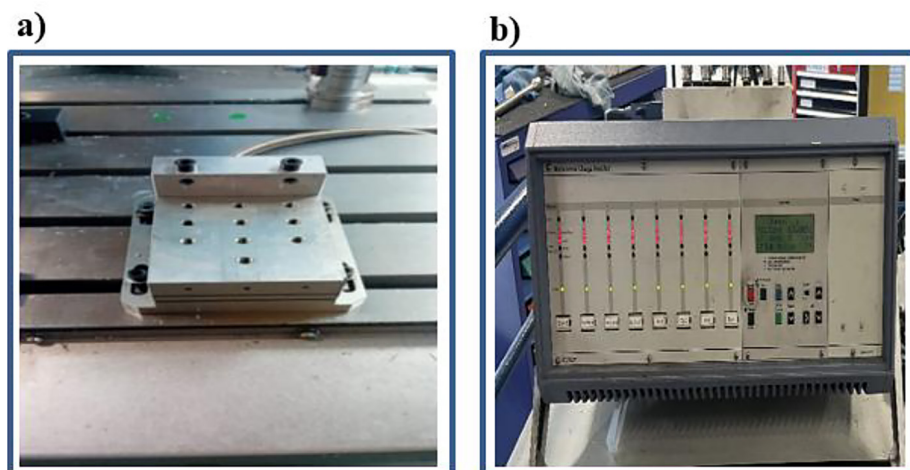


Figure 4. (a) Kistler 9257A dynamometer, (b) Kistler 5017B charge amplifier, TITAN Platform of the UTBM-Industry 4.0 Pole, (Belfort - Montbéliard, France)

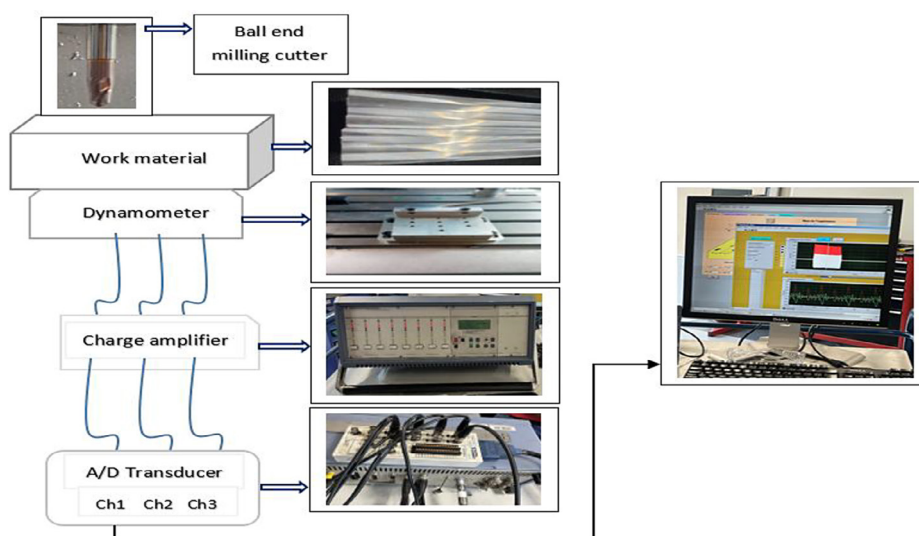


Figure 5. Schematic diagram of cutting force measurements

RESULTS AND VALIDATION

This section presents the cutting forces measured experimentally and predicted via simulation, validating the mechanistic model’s accuracy for ball end milling of aluminum 7075-T6 alloy under the specified conditions.

Experimental force measurements

Force data collected revealed distinct patterns over one revolution, reflecting the flute cutter’s engagement with the workpiece. F_x peaked at approximately 215 N, corresponding to maximum

chip thickness as each flute engaged the material. F_y peaked at 74 N, indicative of lateral forces during entry and exit phases. F_z representing axial loading, reached a maximum of 28 N as seen in Figure 6.

Comparative analysis of measured and predicted cutting forces

A comparison between the predicted and measured cutting forces was performed during the slot milling process over time. This analysis demonstrated the mechanistic model’s ability to effectively capture the dynamics of the high-speed milling operation. While accepted differences

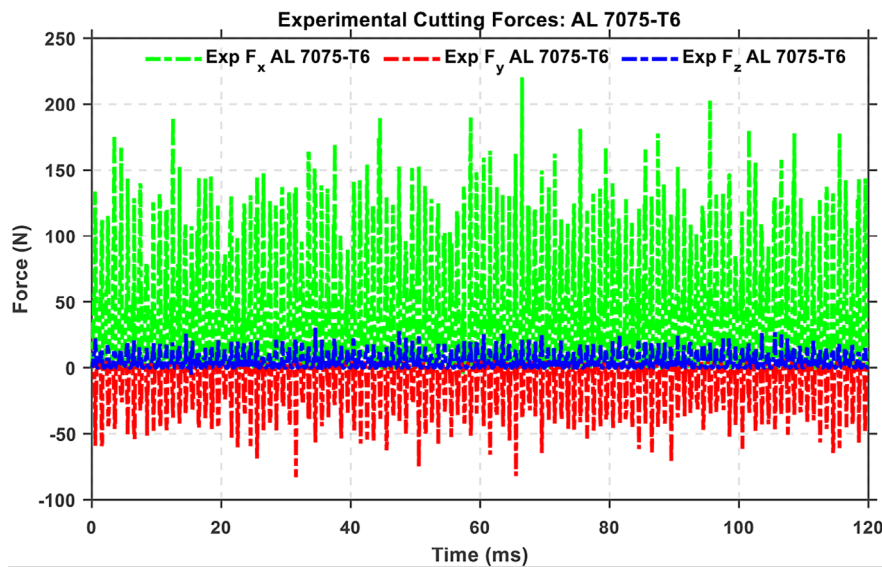


Figure 6. Measured cutting force components for aluminum 7075-T6 alloy

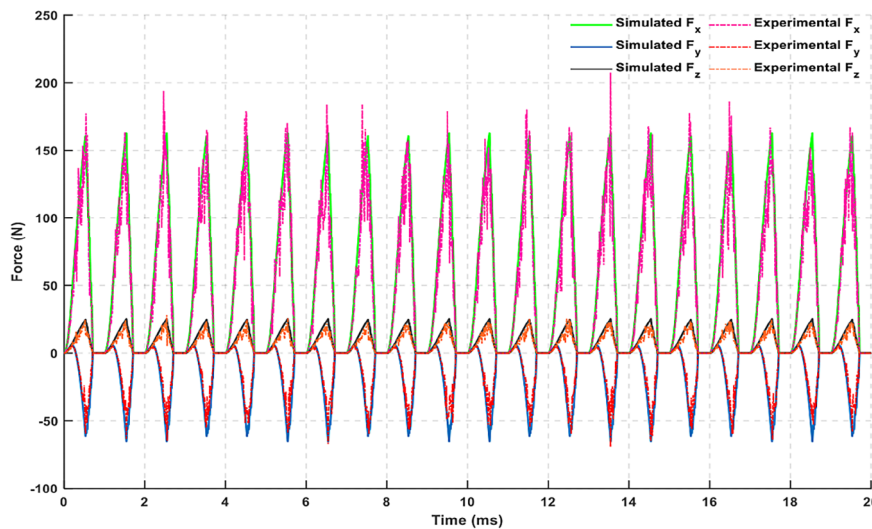


Figure 7. Predicted and measured cutting forces vs. time for slot milling with a 4 fluted ball end mill. Cutting conditions: axial depth of cut = 4 mm, spindle speed = 15000 rpm, helix angle = 30°, feed rate = 3000 mm/min

observed between the predicted and measured forces, particularly at the start and end of the cuts, the overall trends showed strong agreement, confirming the accuracy of the model under the specified cutting conditions, as depicted in Figure 7.

Error analysis: simulated vs. measured cutting forces

In this section, the maximum simulated and measured cutting forces are compared, and the Mean Absolute Error (MAE) is calculated as a percentage to evaluate the error quantitatively. The purpose of this study is to compare the simulation model's accuracy to experimental data in all three directions (x, y and z). Figure 8 displays the maximum simulated and experimental forces alongside their corresponding MAE errors:

- x-direction – simulated force = 162.4 N, experimental force = 215.4 N, MAE = 18.2%
- y-direction – simulated force = 65.2 N, experimental force = 74.3 N, MAE = 4.5%
- z-direction – simulated force = 25.3 N, experimental force = 28.2 N, MAE = 3.3%

The x-direction exhibits the largest discrepancy, with the simulated force under predicting the experimental value by 53.0 N (24.6%), corresponding to an MAE of 18.2%. This indicates that the model may not fully capture the dominant tangential forces, possibly due to simplifications in tool-work piece interaction dynamics or material

specific behavior of aluminum 7075-T6 alloy. In contrast, the y and z-directions show better agreement, with differences of 9.1 N (12.2%) and 2.9 N (10.3%), respectively, and lower MAE values of 4.5% and 3.3%. These results suggest reliable predictions for radial and axial forces.

DISCUSSION

The hybrid mechanistic model developed in this study provides valuable predictions of cutting forces during ball end milling of aluminum 7075-T6 alloy. The mean absolute errors (MAE) were 18.2% in the x-direction, 4.5% in the y-direction, and 3.3% in the z-direction, highlighting both the strengths and limitations of the model. The high accuracy observed in the y and z directions is consistent with previous studies on aluminum alloys, which have reported similar error margins for radial and axial force predictions, confirming the model's reliability in capturing these force dynamics crucial for toolpath optimization and machining stability in aerospace applications [21, 22].

A key parameter in the model is the specific cutting force coefficient ($K_s = 850 \text{ N/mm}^2$), selected based on well-established experimental data for aluminum 7075-T6 alloy [19]. This value effectively represents the material's cutting resistance under typical milling conditions and significantly influences predicted forces. Similar

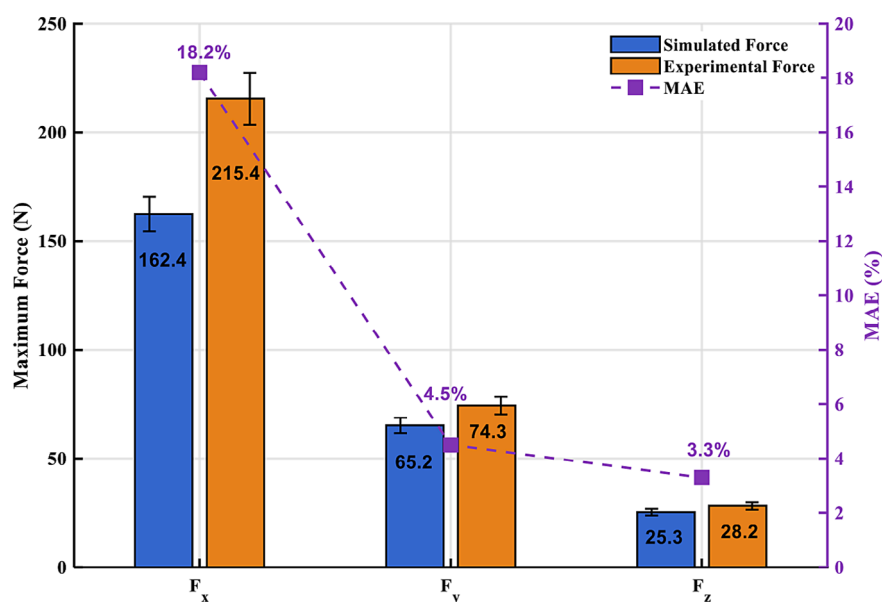


Figure 8. Comparison of maximum simulated and experimental cutting forces with MAE error percentages in high-speed ball-end milling

coefficient values have been reported in prior analytical and experimental studies on aluminum alloys, further validating the parameter selection for this work [23]. While the model performs well in the y and z directions, the higher error in the x-direction suggests that a single K_s value may not fully capture the complexities of tangential forces, which are more sensitive to chip formation and tool engagement [24].

These findings have two major implications: first, the model's accuracy in predicting radial and axial forces makes it a practical tool for enhancing machining efficiency and sustainability in aerospace manufacturing. Second, the relatively large error in the tangential direction points to the need for future refinement, particularly in applications where surface quality and tool wear are critical. This challenge is consistent with observations in the literature, where discrepancies in tangential force prediction have been attributed to tool edge geometry and dynamic effects that are difficult to capture in standard mechanistic models [9].

Further research should focus on improving tangential force modeling, possibly by introducing direction-specific coefficients or dynamic adjustments based on cutting parameters.

CONCLUSIONS

This study successfully develops a hybrid mechanistic model to predict cutting forces in the milling of aluminum 7075-T6 alloy, utilizing a cutting force coefficient ($K_s = 850 \text{ N/mm}^2$) from existing literature. The model demonstrates its effectiveness with a low Mean Absolute Error (MAE) of 18.2% in the x-direction, 4.5% in the y-direction, and 3.3% in the z-direction, confirming its potential for application in high-speed machining scenarios, particularly in the aerospace industry.

The model excels in accurately predicting radial and axial forces (y and z-directions), making it valuable for optimizing machining processes where these force components are critical. However, the model underpredicts the tangential forces in the x-direction, highlighting an area for future refinement, particularly for tasks that demand high precision in all directions of cutting force.

By incorporating the experimentally validated cutting force coefficient, the model is well grounded in real world machining data, ensuring its relevance and precision critical machining operations. Despite the error observed in the

x-direction, the strong performance in the y- and z-directions underscores the model's potential to optimize machining parameters for more efficient and accurate processing of aerospace materials.

This research contributes to the refinement of mechanistic models for high-speed milling, offering a more reliable tool for predicting cutting forces in the milling of aluminum 7075-T6 alloy. The findings emphasize the importance of continual model improvement, particularly in the prediction of tangential forces, to enhance the precision and efficiency of aerospace machining processes.

Acknowledgments

The experimental tests led with the Machining Centre and the acquisition equipment at the TITAN Platform of the UTBM-Industry 4.0 Pole, (France). The authors acknowledge the support extended by Dr. Daniel Schlegel from UTBM (University of Technology of Belfort-Montbéliard) for his assistance in conducting experiments.

REFERENCES

1. Wei Z.C., Guo M.L., Wang M.J., Li S.Q., Wang J. Prediction of cutting force for ball end mill in sculptured surface based on analytic model of CWE and ICCE. *Mach. Sci. Technol.* 2019; 23(5): 688–711. <https://doi.org/10.1080/10910344.2019.1575408>
2. Zhuang K., Yang Y., Dai X., Weng J., Tian C., Gao Z. Multi-axis ball-end milling force prediction model considering the influence of cutting edge. *Int. J. Adv. Manuf. Technol.* 2023; 128: 357–371. <https://doi.org/10.1007/s00170-023-11890-4>
3. Mou W., Zhu S., Zhu M., Han L., Jiang L. A prediction model of cutting force about ball end milling for sculptured surface. *Math. Probl. Eng.* 2020; 2020: 1389718. <https://doi.org/10.1155/2020/1389718>
4. Wang H., Tao K., Jin T. Modeling and estimation of cutting forces in ball helical milling process. *Int. J. Adv. Manuf. Technol.* 2021; 117(9): 2807–2818. <https://doi.org/10.1007/s00170-021-07817-6>
5. Nguyen V.H., Le T.T. Predicting surface roughness in machining aluminum alloys taking into account material properties. *Int. J. Comput. Integr. Manuf.* 2024. <https://doi.org/10.1080/0951192X.2024.2372252>
6. Yue Q., He Y., Li Y., Tian S. Modeling and optimization of surface residual stress profiles in milling of aluminum 7075-T6 alloy. *Int. J. Adv. Manuf. Technol.* 2024; 130(11): 5913–5934. <https://doi.org/10.1007/s00170-024-13057-1>
7. Xu, Y., Yue, C., Chen, Z., Li, M., Wang, L., Liu, X.

- Finite element simulation of residual stress in milling of aluminum alloy with different passes. *International Journal of Advanced Manufacturing Technology*, 127(9–10), 4199–4210, 2023. <https://doi.org/10.1007/s00170-023-11795-2>
8. Duan, Z., Li, C., Ding, W., Zhang, Y., Yang, M., Gao, T., Cao, H., Xu, X., Wang, D., Mao, C., Li, H. N., Kumar, G. M., Said, Z., Debnath, S., Jamil, M., Hafiz, M. A. Milling force model for aviation aluminum alloy: Academic insight and perspective analysis. *Chinese Journal of Mechanical Engineering*, 34, Article number: 18, 2021. <https://doi.org/10.1186/s10033-021-00536-9>
 9. Bahram M. Unified mechanistic identification of cutting force coefficients. Master's thesis, The University of British Columbia (Vancouver), Canada, May 2023. <https://open.library.ubc.ca/soa/cIRcle/collections/ubctheses/24/items/1.0432479>
 10. Dikshit M.K. Determination of force coefficient based on instantaneous forces and linear mechanistic model in ball end milling. *Proc. Inst. Mech. Eng. Part B J. Eng. Manuf.* 2022; 237(11): 2070–2082. <https://doi.org/10.1177/09544054221136515>
 11. Wang Z., Cao Y., Yao H., Kou F. Dynamic simulation and experimental study of cutting force by rake angle of multi-axis high-speed ball-end milling tool. *Int. J. Adv. Manuf. Technol.* 2022; 122: 377–390.
 12. Wang R., Zhang S., Ge R., Luan X., Wang J., Lu S. Modified cutting force prediction model considering the true trajectory of cutting edge and in-process workpiece geometry in ball-end milling operation. *Int. J. Adv. Manuf. Technol.* 2021; 115(4): 1187–1199. <https://doi.org/10.1007/s00170-021-07285-y>
 13. Qin S., Hao Y., Zhu L., Wiercigroch M., Yuan Z., Shi C., Cui D. CWE identification and cutting forces prediction in ball-end milling process. *Int. J. Mech. Sci.* 2023; 239: 107863. <https://doi.org/10.1016/j.ijmecsci.2022.107863>
 14. Li F., Liu J., Hu B., Jin H. An optimized method for calibration milling force coefficients and cutter run-out parameters in end milling process. *Int. J. Adv. Manuf. Technol.* 2024; 135(5–6): 2597–2606. <https://doi.org/10.1007/s00170-024-14620-6>
 15. Nan C., Liu D. Analytical calculation of cutting forces in ball-end milling with inclination angle. *J. Manuf. Mater. Process.* 2018; 2(2): 35. <https://doi.org/10.3390/jmmp2020035>
 16. Calleja A., Alonso M.A., Fernández A., Tabernero I., Ayesta I., Lamikiz A., López de Lacalle L.N. Flank milling model for tool path programming of turbine blisks and compressors. *Int. J. Prod. Res.* 2015; 53(11): 3346–3362. <https://doi.org/10.1080/00207543.2014.983619>
 17. Miao H., Wang C., Li C., Yao G., Zhang X., Liu Z., Xu M. Dynamic modeling and nonlinear vibration analysis of spindle system during ball end milling process. *Int. J. Adv. Manuf. Technol.* 2022; 121(11): 7867–7889. <https://doi.org/10.1007/s00170-022-09759-1>
 18. Cai S., Cai Z., Yao B., Shen Z., Ma X. Identifying the transient milling force coefficient of a slender end-milling cutter with vibrations. *J. Manuf. Process.* 2021; 67: 262–274. <https://doi.org/10.1016/j.jmapro.2021.05.025>
 19. Schmitz T.L., Smith K.S. *Machining Dynamics: Frequency Response to Improved Productivity*. Springer, 2019. <https://link.springer.com/book/10.1007/978-3-319-93707-6>
 20. Rebai S. L'influence de la direction d'usinage sur le comportement dynamique du processus de fraiseage. Master's thesis, Université Mohamed Khider - Biskra, Algeria, 2015. <http://archives.univ-biskra.dz/handle/123456789/24829>
 21. Sethupathy A., Shanmugasundaram N. Prediction of cutting force based on machining parameters on AL7075-T6 aluminum alloy by response surface methodology in end milling. *Mater. Werkst. Tech.* 2021; 52(8): 879–890. <https://doi.org/10.1002/mawe.202000086>
 22. Zhou M., Chen Y., Zhang G. Force prediction and